

SUPPLEMENTARY INFORMATION

Enhancing chemical signal transformation in lateral flow assays using aptamer-architected plasmonic nanozymes and para-phenylenediamine

Elangovan Sarathkumar¹, Kunnumpurathu Jibin¹, Subramani Sivaselvam¹, Arumugam Selva Sharma², Vincent Alexandar³, AN Resmi¹, Poornima Velswamy⁴, Ramapurath S.Jayasree^{1*}

¹Division of Biophotonics and Imaging, Biomedical Technology Wing, Sree Chitra Tirunal Institute for Medical Sciences and Technology, Poojappura, Thiruvananthapuram-695012, Kerala, India.

²Department of Nanoscience and Technology, Gachon University, 1342 Seongnam-daero, Sujeong-gu, Seongnam-si, Gyeonggi-do 13120, South Korea.

³Institute of Systems, Molecular and Integrative Biology, University of Liverpool, Liverpool, United Kingdom.

⁴Department of Pharmacology and Therapeutics, University of Liverpool, Liverpool, United Kingdom.

E-mail: Ramapurath S. Jayasree* - jayasree@sctimst.ac.in - jayashreemenon@gmail.com

*Corresponding author

S1. Materials and Methods

S1.1. Materials and Reagents

Gold chloride ($\text{HAuCl}_4 \cdot 3\text{H}_2\text{O}$), Sodium citrate, recombinant SARS-CoV-2 spike protein, Bovine serum albumin (BSA), HRP-Streptavidin, Para-phenylenediamine (PPD) and Human serum albumin (HSA) were purchased from Sigma Aldrich. Nitrocellulose membrane, cellulose sample pad, glass fiber membranes were purchased from Advanced Microdevices, Pvt Ltd, India. The aptamer 51 and aptamer 67 were procured from Eurofins Genomics, Pvt Ltd, India. The sequences of aptamers used in this work are provided in the Table S1. All other chemicals employed in this study were of analytical grade and used without purification.

S1.2. Instrumentation

The surface functionalities of the nanomaterials were determined by Fourier Transform Infrared spectrometer (Agilent, Cary 600 series) using ATR mode within the wave number region of $4000\text{--}500\text{ cm}^{-1}$. High resolution transmission electronmicroscopy (JEOL JEM, 2100) operating

at 200 kV was used to record the size and morphology of the GNPs. The optical absorbance of the sample was recorded using UV-Vis spectroscopy at room temperature (UV-1800 Shimadzu). The elemental composition of the GNPs was identified using X-ray photoelectron spectroscopy (K-Alpha Surface Analysis, Thermo Scientific) operating at room temperature with Al K α radiation as an X-ray source. The Dynamic light scattering analysis (DLS) was performed in Malvern particle size analyzer. The concentration of GNPs is determined using ICP-OES (Agilent 5110).

S1.3. Synthesis of GNPs

The GNPs were synthesized using the sodium citrate reduction method, as previously reported, with some modifications. Briefly, 100 μ L of H₂AuCl₄·3H₂O (0.1 M) was added to distilled water (50 mL) under vigorous stirring. Gradually, the temperature of the above solution was increased to 85° C followed by addition of 100 μ L of trisodium citrate (0.1 M). The solution was stirred at 85° C for 2 h. After the solution reached room temperature, the GNPs were separated by centrifugation (10000 rpm, 10 min) and washed thrice with distilled water. The prepared GNPs were stored at 4° C for further use.

S1.4. Molecular dynamic simulation study

The UNA fold web server was employed to predict the secondary structure of aptamer 51 and aptamer 67 based on their Gibbs free energy values. Subsequently, the RNA composer tool was employed to generate the tertiary structure of the aptamer, by converting DNA to RNA sequence by manually substituting the Uracil (U) bases with Thymine (T). The tertiary structure of the SARS-CoV-2 spike protein was obtained from the RCSB PDB data bank (ID: 6VXX). Molecular docking between the 3D structures of the aptamers and the SARS-CoV-2 spike protein was performed using the Patchdock server, with default values for the molecular docking parameters as specified on the website.

S1.5. *In-Vitro* binding study of aptamer using dot blot assay

To assess the binding efficacy of aptamer 51, it was exposed to folding buffer at 85° C and then immediately cooled to 37° C on ice to maintain its structural conformation. Initially, 2 μ L of aptamer 51 (1 μ M) was drop casted to the nitrocellulose membrane and dried at room

temperature for 4 hours. Then, COVID-19 spike protein (1 μ L, 1 μ g/mL) was added to the immobilized aptamer after blocking the membrane with 5 μ L of 0.05% BSA. Following 1 h of incubation, the unbound proteins were removed by gently immersing into PBS wash and incubated with 2 μ L of biotin-terminated aptamer 67 (0.1 - 0.01 μ M) for 60 min. After a gentle wash with PBS, the membrane was subsequently added with 3 μ L of HRP streptavidin at a concentration of 0.5 μ g/mL for 30 minutes and washed with PBS. Finally, 5 μ L of peroxidase substrate TMB/H₂O₂ (2mM/50mM) was added to the aptamer-protein complex, and the formation of Oxy-TMB (blue color) could be observed by the naked eye. A control sample was also prepared using the same parameters except COVID-19 spike protein addition.

S1.6. *In-Vitro* binding study of aptamer using aptamer lateral flow assay

The GNPs were conjugated with COVID-19 spike protein *via* adsorption by mixing 10 μ L of 10 μ M spike protein with 1 mL of GNPs for 2 hours in PBS at pH 6.0. Unbound sites in the GNPs were blocked using Tween 20 (0.01%) and BSA (0.1%). Following a one hour incubation, the solution was washed and dispersed in 100 μ L of MilliQ water. To perform the LFA assay, nitrocellulose membrane (10 μ m, pore size) containing streptavidin (1 μ L, 0.5 μ g/mL) was affixed with 1 μ L of biotin-terminated aptamer 67 (10 μ M) and incubated for 4 hours. Then, 10 μ L of spike protein conjugated GNP was loaded on the conjugate pad, dried at 30°C for 2 hours, and assembled with LFA strips. The sample was run using a PBS running buffer containing Tween 20 (0.01%) and BSA (0.1%). A control sample was also prepared using GNPs without spike protein. Finally, the color intensity on the test spot was measured using ImageJ software.

S1.7. Functionalization of GNP with aptamer 51

The GNP was functionalized with carboxylated group using 16-mercaptohexadecanoic acid (16-MHDA) by adding 50 μ L of 16-MHDA (10 mM) to 950 μ L of GNP followed by incubation at room temperature for 20 min. The mixture was added with Tween 20 (0.01%) and BSA (0.1%). After incubation for 2 h, the sample was washed and dispersed in 500 μ L of PBS at pH 6.0. The conjugation of carboxylated GNP and aptamer 51 was performed using the EDC and NHS chemistry. Briefly, 60 μ L of EDC (50 mM) and NHS (25 mM) were added to 500 μ L of carboxylated GNP and incubated for 8 h. Then amine terminated aptamer 51 (10 μ L, 10 μ M), which was heated to 85°C for 5 minutes and snap-chilled on ice to 37°C to preserve its structural

integrity, was quickly added to the above mixture and left overnight under stirring. Finally, the solution was washed and the pellet was redispersed in 100 μL of MilliQ water.

S1.8. Detection of COVID-19 spike protein using PPD based LFA

The GNP functionalized aptamer 51 (20 μL) was affixed to the conjugation pad and dried in oven at 37° C for 15 min. The aptamer 67 (1 μL , 10 μM) was then affixed to the test line and the LFA test strip was assembled in the order of conjugation pad, sample pad and adsorbent pad. The COVID-19 spike protein was diluted into different concentration (0.1 to 50 ng mL^{-1}) in the PBS running buffer and was added to the sample pad. For each LFA strip, 200 μL of running buffer containing different concentrations of spike protein was used. The LFA strip was left undisturbed for 10 min. Then, 1 μL of peroxidase substrate PPD/ H_2O_2 was added to the test line and the results were visualized after 10 min of incubation. To reduce background signal, the test signal was subtracted from the unspiked sample, which was used as the background. By varying the concentration of spike protein, the LOD was determined. The limit of detection (LOD) was calculated using the formula: $\text{LOD} = 3 \times (\text{SD} / \text{slope})$ where SD is the standard deviation of the blank (unspiked sample) and the slope is derived from the calibration curve of the assay. The optimum concentration of PPD and H_2O_2 used in this study were also optimized. The selectivity of the prepared LFA on COVID-19 spike protein was examined using different interference agents such as, BSA, HSA, MERS-S1 and Rhinovirus.

S1.9. Protein spiked and Clinical sample analysis

For the protein spiked sample analysis, nasopharyngeal (NPh) swab samples were collected from the healthy volunteers and it is placed in the polypropylene tube containing lysis buffer. The samples were diluted in a 1:1 ratio with running buffer before spiking with different concentrations of COVID-19 spike protein (100-2000 pg/mL). The LFA assay was then performed, and the recovery percentage was calculated using the following formula:

$$\text{Recovery (\%)} = [(\text{Measured concentration of spiked sample} - \text{Measured concentration of unspiked sample}) / \text{Spike protein concentration added}] \times 100$$

In order to validate the performance of LFA strips clinical samples from suspected individuals were collected and RT-PCR analysis were performed to segregate positive and negative samples.

The samples were placed in the polypropylene tube containing lysis buffer for 10 min, then diluted with 1:1 ratio with running buffer before LFA analysis. The results were compared with commercially available LFA kits.

S1.10. Statistical analysis

The resulting image of the LFA test line were quantified by using ImageJ IJ 1.46r (National Institutes of Health, Maryland, USA) software. For each image, the region of interest (ROI) in the test line was selected and the RGB value was computed. The mean value of the samples was compared with the control sample using ANOVA followed by a Bonferroni post hoc test using IBM SPSS software (IBM Corporation, USA). The error bars indicate the standard deviation (SD) of 6 independent experiments.

S2. Mobile app development

COVID-19 spike protein quantification was carried out with the in-house developed software application using the integrated development environment (IDE) for Android OS. The application is designed for colorimetric analysis which could be operated at all time and place as required. The application is designed for image acquisition, data preparation, data analysis and to produce results which in turn could be stored for future reference. The application is calibrated with the samples containing known concentrations of the protein. The calibration curve was prepared from COVID-19 spike protein concentration to test spot intensity, the region in which linearity was obtained for the measurements. As you start the app upon installation, the home page opens with the display and option for image capturing. The image capturing region contains the guidance grid for placing the LFA strip. The focus region of the grid consists of two main points namely the cross hairs to focus the spot intensity (the test region) and another parallel point for background capture. The background capture is performed in order to alleviate any hindrances/noise that might be produced during sample analysis.

S2.1. Sample analysis with Smartphone

Real time sample analysis is carried out using the mobile camera (**Figure S9**). The mobile camera was positioned at a distance of 20 cm from the LFA test strip, and an ambient light condition was utilized to capture the images. The test zone signal intensity is calculated by

subtracting the background signal near the test spot from each test strip using the mobile application. Sample analysis is carried out based on the RGB_{AVG} . In order to, maintain the uniformity of the sample analysis a 50 * 50-pixel region at the center of the test spot is chosen as the region of interest (ROI) for further analyses. The calibration curve obtained with the mobile application agrees with that obtained using the gold standard. In addition, smartphone assisted detection was found to be more sensitive as compared to the traditional methods, thereby facilitating the early onset of infection. Clinical sample analysis performed using the mobile application provided convincing results and can be used for semi-quantitative detection.

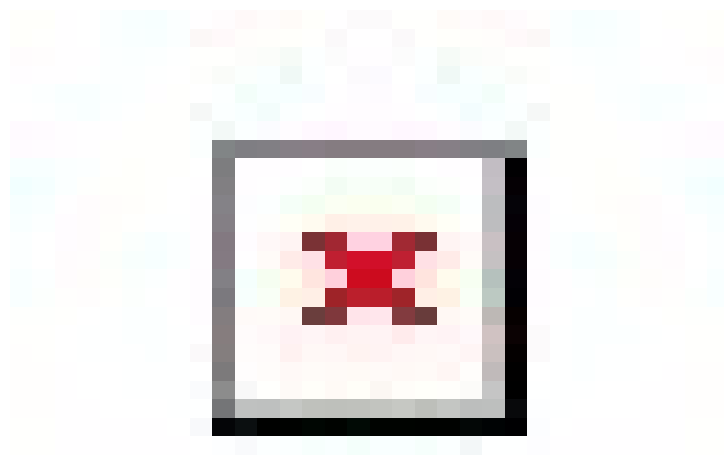


Figure S1. Catalytic activity of GNP on TMB substrate at different pH. The Error bar represents the SD of measurement from six independent strips.

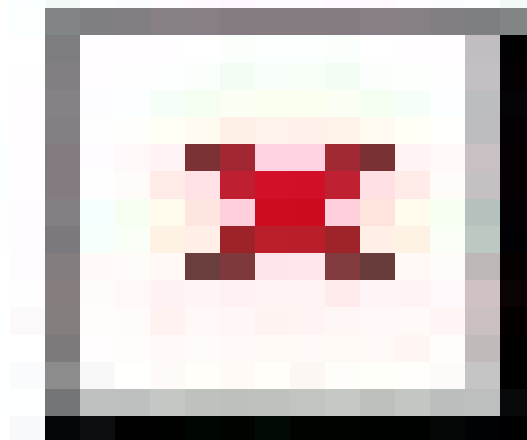


Figure S2. Nanozymatic activity of GNP on TMB as chromogenic substrate. Optimization of (a) Time and (b) TMB concentration. (c) Plot of initial velocity (V) against TMB concentration and (d) double-reciprocal plot generated from (c). The error bar represents the SD of measurement from three independent strips.

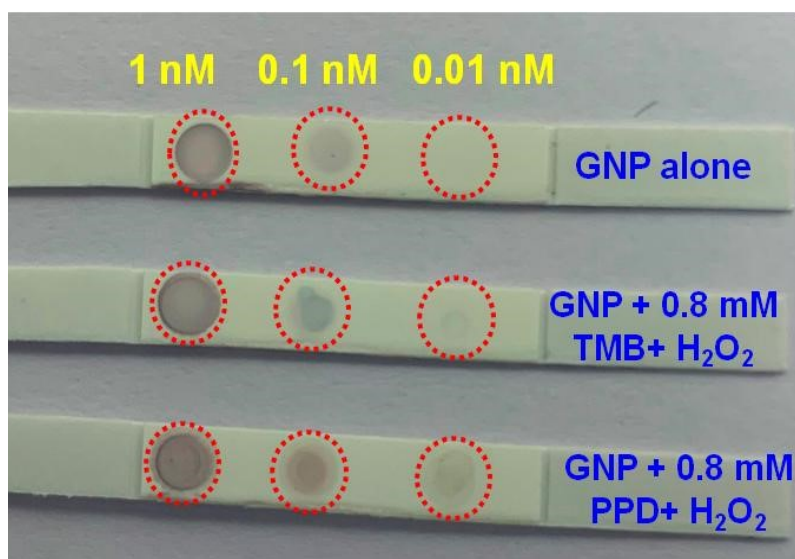


Figure S3. Signal enhancement of two different chromogenic substrate (TMB and PPD) on catalytic activity of GNPs in the nitrocellulose membrane

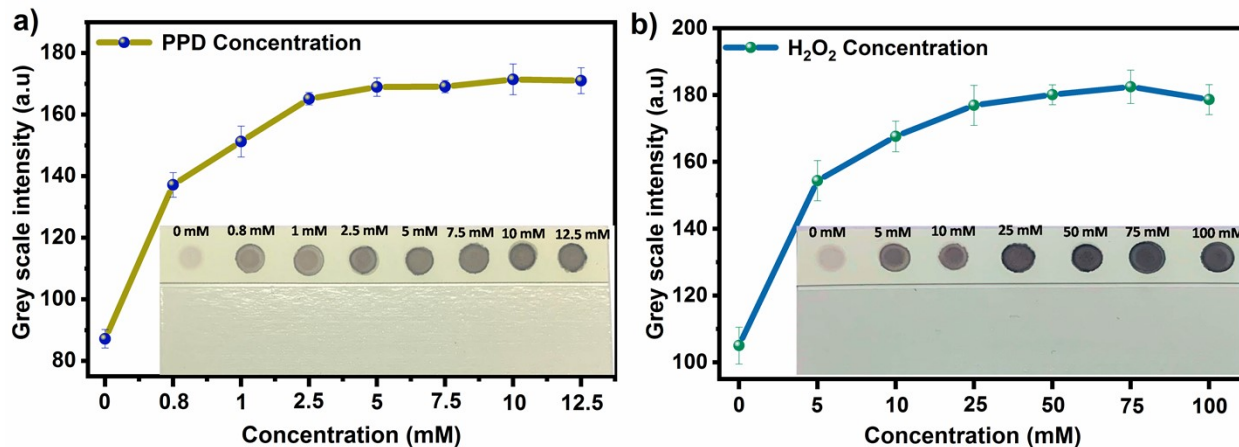


Figure S4. Optimization of (a) PPD and (b) H₂O₂ concentration in the nitrocellulose membrane. The error bar indicates the SD of measurements from three independent strips

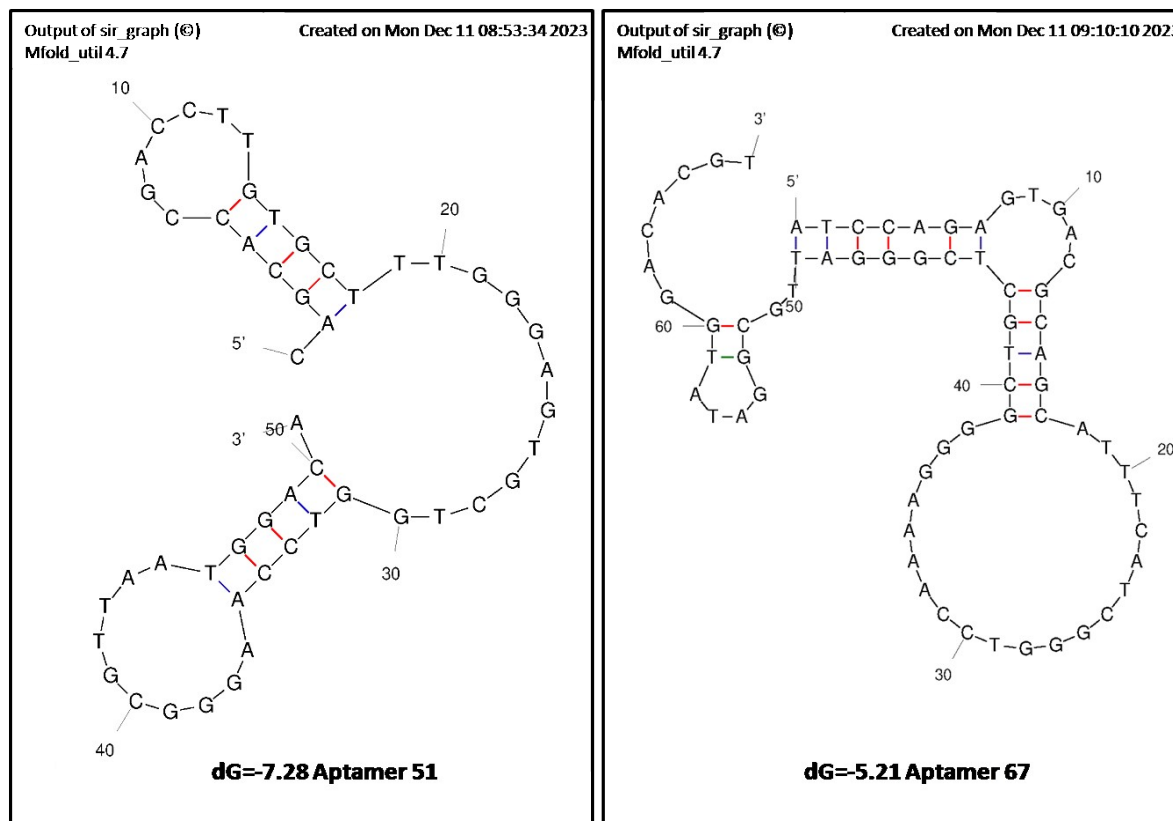


Figure S5. Secondary structure of Aptamer 51 and aptamer 67

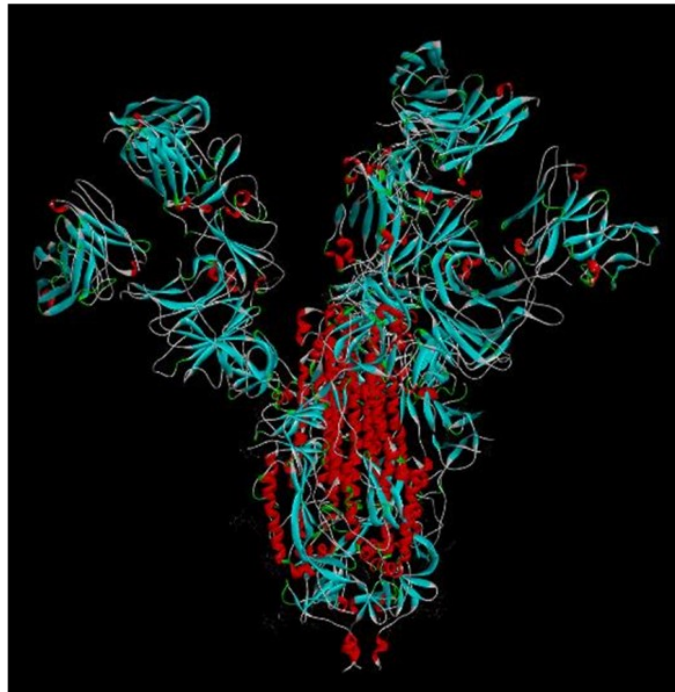


Figure S6. Tertiary structure of COVID-19 spike protein

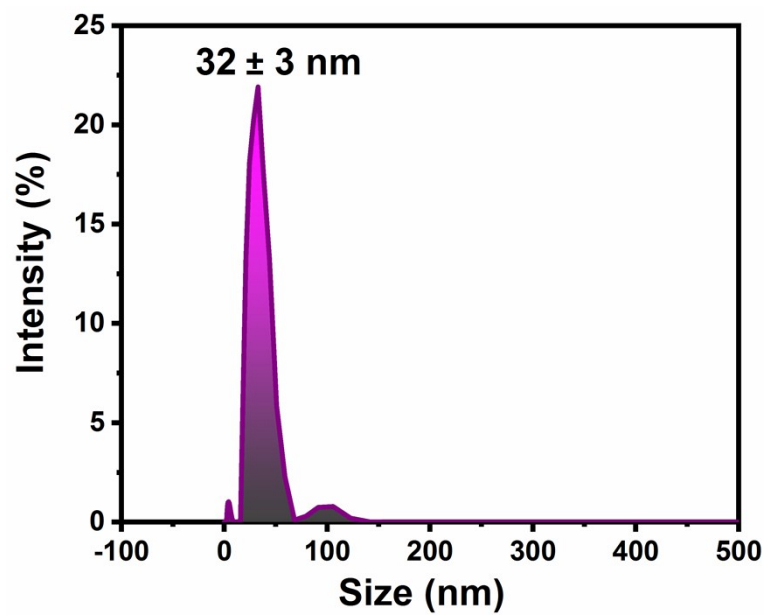


Figure S7.DLS showing hydrodynamic size of aptamer 51 functionalized GNPs.

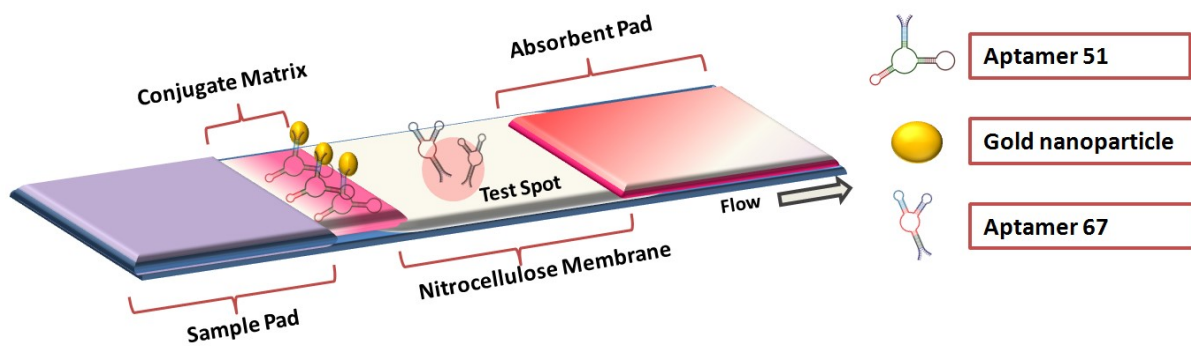


Figure S8. Lateral flow assay test strip construction

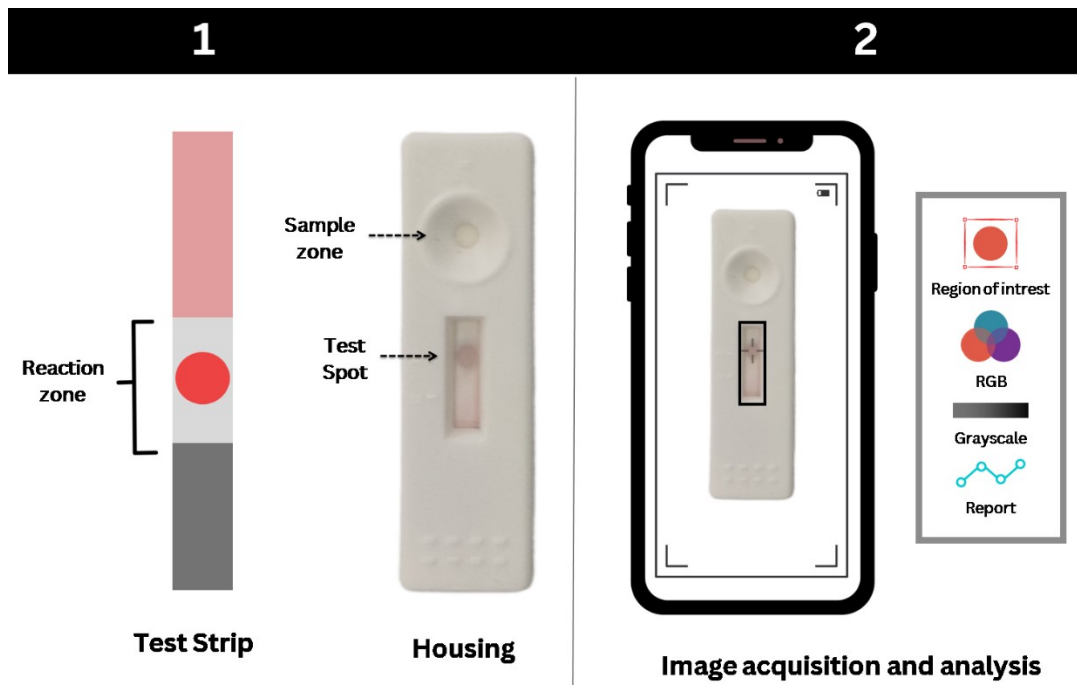


Figure S9. Smart phone based image acquisition and analysis

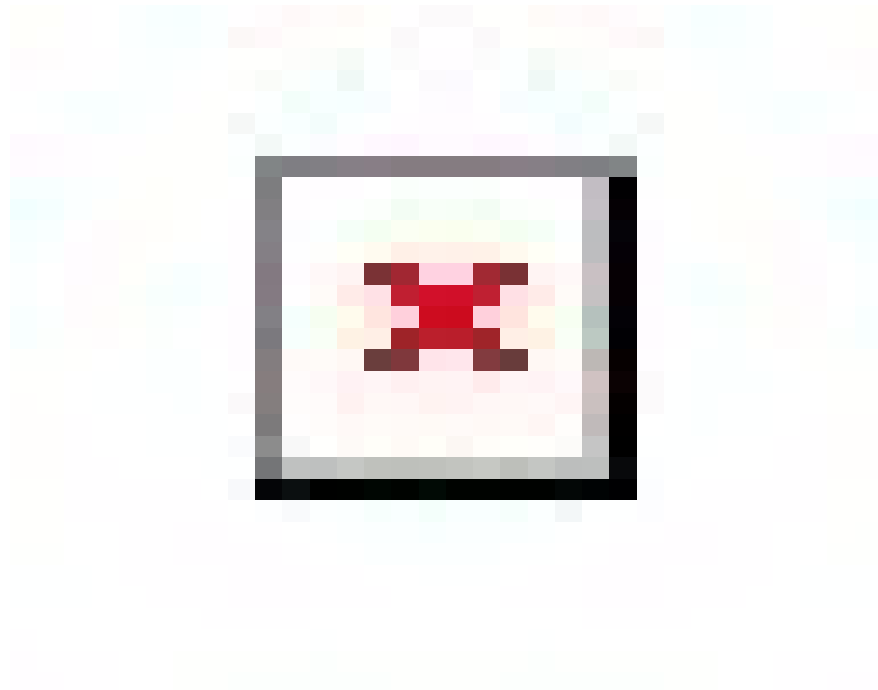


Figure S10. Correlation analysis between the quantification of signal intensity in LFA strips between Image J and Mobile app

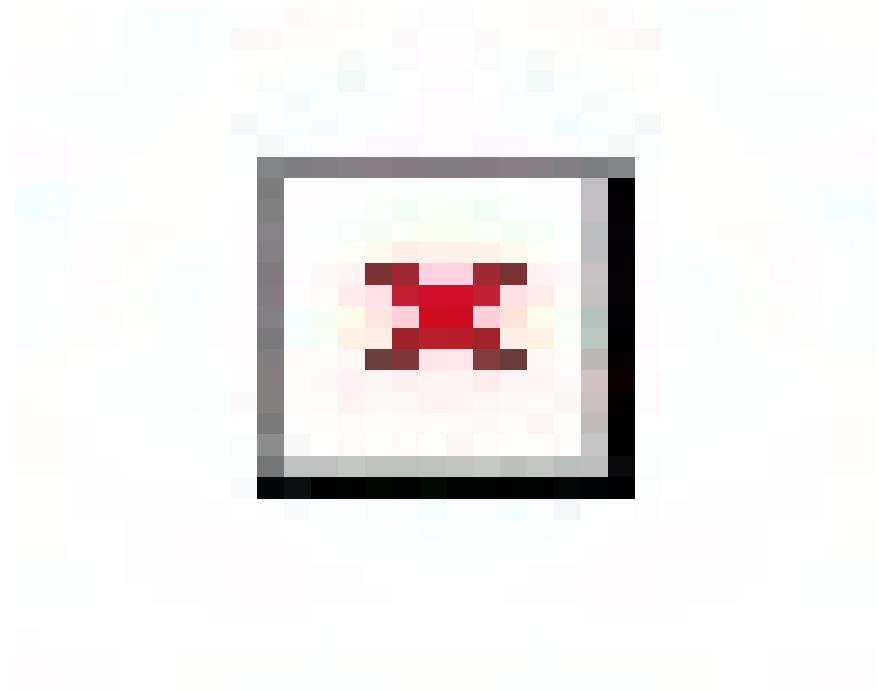


Figure S11. Correlation analysis of the quantifying spike protein concentration in NPh sample by ELISA and developed mobile app

Table S1. The aptamer sequences used in this study

Aptamer 51	5'- CAGCACCGACCTTGTGCTTTGGGAGTGCTGGTCCAAGGG CGTTAATGGACA-3'	1
Aptamer 67	5'- ATCCAGAGTGACGCAGCATTTCATCGGGTCCAAAAGGGG CTGCTCGGGATTGCGGATATGGACACGT-3'	1

Table S2. Catalytic activity of GNPs on TMB and PPD as substrates, compared to the standard HRP

Catalyst	Substrate	Vmax	Km	K_{cat}	Ref
15 nm GNPs	TMB	3.73×10^{-6}	0.2 mM	1.041×10^6	This work
HRP	TMB	10×10^{-8}	0.434 mM	4.3×10^3	2
15 nm GNPs	PPD	1.04×10^{-7}	0.6 mM	2.905×10^4	This Work
HRP	PPD	53.2×10^{-8}	0.92 mM	0.106×10^4	3

Table S3. Comparison of the Limit of Detection of LFA-Based SARS-CoV-2 Spike Protein with Reported Literature

S.No	Detection Method	Target	Recognition Element	LOD (ng/mL)	Time (min)	Ref
1	Fluorescence	Spike protein and nucleocapsid protein	Antibodies	2.2	10	4
2	Chemiluminescence	Spike protein	Antibodies	0.1	16	5
3	Colorimetric	Spike protein	Antibodies	0.11	15	6
4	Colorimetric	Nucleocapsid protein	Antibodies	0.65	20	7
5	Colorimetric	spike protein	Antibodies	0.625	15 - 30	8

6	Colorimetric	Nucleocapsid protein	Antibodies	2	20	⁹
7	Fluorescence	Nucleocapsid protein	Antibodies	0.1	20	¹⁰
8	SERS	IgG	Antibodies	0.1	-	¹¹
9	Fluorescence	Nucleocapsid protein	Antibodies	0.12	10	¹²
10	Fluorescence	Spike protein and Nucleocapsid protein	Antibodies	7.2	20	¹³
11	Colorimetric	Spike protein	Aptamers	0.16	10	This work

Table S4. Detection of COVID-19 spike protein in the real patient sample.

Sample ID	CT Value (orf gene)	CT Value (N gene)	Average CT value	LFA test intensity	LFA result Positive/Negative	LFA concentration (pg/mL)
98	17.87	16.91	17.39	113.78	Positive	>2000
99	20.62	17.67	19.145	106.28	Positive	>2000
150	19	15.1	17.05	108.782	Positive	>2000
177	18.56	16.77	17.665	122.611	Positive	>2000
200	18.88	20.03	19.455	97.15	Positive	≤2000
212	19.05	16.81	17.93	102.92	Positive	>2000
217	18.08	15.09	16.585	134.64	Positive	>2000
259	19.2	18.66	18.93	79.28	Positive	1099.15
312	20.4	20.07	20.235	80.69	Positive	1193.22
365	20.66	18.16	19.41	93.47	Positive	2045.42
372	14.32	16.64	15.48	151.42	Positive	>2000
400	19.24	18.12	18.68	109.41	Positive	>2000
162	24.29	22.54	23.415	72.57	Positive	616.28
165	25.15	21.04	23.095	75.60	Positive	650.18
185	24.08	22.05	23.065	78.70	Positive	721.5

215	22.17	19.28	20.725	78.10	Positive	718
249	22.04	22.58	22.31	70.15	Positive	592
250	26.8	25.35	26.075	56.75	Negative	<100
299	23.54	23.02	23.28	67.61	Positive	320
311	23.51	23.18	23.345	67.80	Positive	344
327	21.11	20.28	20.695	89.80	Positive	1800.76
381	24.05	23.05	23.55	70.319	Positive	500.96
457	23.43	18.29	20.86	97.31	Positive	≤2000
470	25.78	24.93	25.355	62.05	Negative	<200
507	21.41	21.07	21.24	78.131	Positive	724.54

References

- 1 Y. Song, J. Song, X. Wei, M. Huang, M. Sun, L. Zhu, B. Lin, H. Shen, Z. Zhu and C. Yang, *Anal Chem*, 2020, **92**, 9895–9900.
- 2 L. Wu, G. Wan, N. Hu, Z. He, S. Shi, Y. Suo, K. Wang, X. Xu, Y. Tang and G. Wang, *Nanomaterials* 2018, Vol. 8, Page 451, 2018, **8**, 451.
- 3 Y. Zhang, Y. R. F. Schmid, S. Luginbühl, Q. Wang, P. S. Dittrich and P. Walde, *Anal Chem*, 2017, **89**, 5484–5493.
- 4 J. Guo, S. Chen, S. Tian, K. Liu, J. Ni, M. Zhao, Y. Kang, X. Ma and J. Guo, *Biosens Bioelectron*, 2021, **181**, 113160.
- 5 D. Liu, C. Ju, C. Han, R. Shi, X. Chen, D. Duan, J. Yan and X. Yan, *Biosens Bioelectron*, 2021, **173**, 112817.
- 6 P. Srithong, S. Chaiyo, E. Pasomsub, S. Rengpipat, O. Chailapakul and N. Praphairaksit, *Microchimica Acta*, 2022, **189**, 1–10.
- 7 B. D. Grant, C. E. Anderson, J. R. Williford, L. F. Alonzo, V. A. Glukhova, D. S. Boyle, B. H. Weigl and K. P. Nichols, *Anal Chem*, 2020, **92**, 11305–11309.
- 8 G. Li, A. Wang, Y. Chen, Y. Sun, Y. Du, X. Wang, P. Ding, R. Jia, Y. Wang and G. Zhang, *Front Immunol*, 2021, **12**, 635677.
- 9 H. Y. Kim, J. H. Lee, M. J. Kim, S. C. Park, M. Choi, W. Lee, K. B. Ku, B. T. Kim, E. Changkyun Park, H. G. Kim and S. Il Kim, *Biosens Bioelectron*, 2021, **175**, 112868.

- 10 L. Di Xu, J. Zhu and S. N. Ding, *Analyst*, 2021, **146**, 5055–5060.
- 11 S. Chen, L. Meng, L. Wang, X. Huang, S. Ali, X. Chen, M. Yu, M. Yi, L. Li, X. Chen, L. Yuan, W. Shi and G. Huang, *Sens Actuators B Chem*, 2021, **348**, 130706.
- 12 Z. Xie, S. Feng, F. Pei, M. Xia, Q. Hao, B. Liu, Z. Tong, J. Wang, W. Lei and X. Mu, *Anal Chim Acta*, 2022, **1233**, 340486.
- 13 G. Q. Zhang, Z. Gao, J. Zhang, H. Ou, H. Gao, R. T. K. Kwok, D. Ding and B. Z. Tang, *Cell Rep Phys Sci*, 2022, **3**, 100740.